Jan-Yves Ruzicka, Faridah Abu Bakar, Christoffer Hoeck, Rohul Adnan, Campbell McNicoll, Tim Kemmitt, Bruce C. Cowie, Gregory F. Metha, Gunther G. Andersson, and Vladimir B. Golovko
Toward control of gold cluster aggregation on TiO_2 via surface treatments
Journal of Physical Chemistry C, 2015; 119(43):24465-24474

Published version http://dx.doi.org/10.1021/acs.jpcc.5b07732

THE JOURNAL OF PHYSICAL CHEMISTRY C

Article

pubs.acs.org/JPCC

Toward Control of Gold Cluster Aggregation on TiO_2 via Surface Treatments

Jan-Yves Ruzicka,[†] Faridah Abu Bakar,[†,‡] Christoffer Hoeck,[†,§] Rohul Adnan,[†,∥] Campbell McNicoll,[†,⊥,#] Tim Kemmitt,[⊥,#] Bruce C. Cowie,[¶] Gregory F. Metha,[*,○] Gunther G. Andersson,[*,◆] and Vladimir B. Golovko[*,†,#]

[†]Department of Chemistry, University of Canterbury, Christchurch 8041, New Zealand

[‡]Universiti Tun Hussein Onn Malaysia, Batu Pahat 86400, Malaysia

[§]University of Copenhagen, Copenhagen, Denmark

[∥]Chemistry Department, University of Malaya, Kuala Lumpur 50603, Malaysia

[⊥]Callaghan Innovation, Lower Hutt 5040, New Zealand

[#]MacDiarmid Institute for Advanced Materials and Nanotechnology, Wellington 6140, New Zealand

[¶]Australian Synchrotron, Clayton, VIC 3168, Australia

[○]Department of Chemistry, University of Adelaide, Adelaide, South Australia 5005, Australia

[◆]Flinders Centre for NanoScale Science and Technology (CNST), Flinders University, Adelaide 5042, Australia

Supporting Information

ABSTRACT: Well-defined Au−TiO_2 materials were synthesized by deposition of triphenylphosphine-protected Au_9 clusters on TiO_2 (Aeroxide P-25), pre-treated in eight different ways and subsequently exposed to two post-treatments. X-ray photoelectron spectroscopy and UV−vis diffuse reflectance spectroscopy studies showed that in most cases the PPh_3 ligand shell was removed upon deposition even before post-treatment, coinciding with some cluster aggregation. However, clusters deposited on TiO_2 treated using H_2SO_4 and H_2O_2 showed remarkable resistance to aggregation, even after high-temperature calcination, while clusters on H_2-treated TiO_2 showed the greatest resistance to aggregation under ozonolysis.

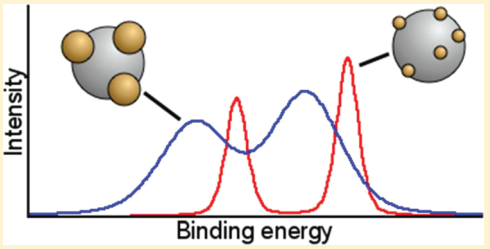

INTRODUCTION

It is well-known that the properties of metal oxide surfaces can be modified by the deposition of Au clusters.[1−4] Pure metal clusters can be generated and deposited from the gas phase as size-selected clusters, while ligand-protected, chemically synthesized clusters could be deposited either through electrospray ionization[5] or from the liquid phase (solutions) by using dip-, drop-, or spin-coating techniques.[6,7] Liquid-phase chemical synthesis of metal clusters allows for excellent control over particle composition and size, while offering benefits of the large-scale production difficult to achieve by gas-phase techniques.[6,8] However, stabilizing ligands must be used to control particle growth, prevent aggregation, and ensure solubility in the reaction media. Once the ligand-stabilized clusters are deposited on a support, the ligands can be removed via heating, facilitating the direct contact of the cluster core with the substrate.[6,9,10] Thermal (calcination)[6,9−12] and oxidative (ozonolysis)[12,13] treatments are often used to remove stabilizing ligands and also help anchor the particles to the support,[6,9,10,12,13] minimizing cluster sintering during catalysis. Avoiding the latter is critical since properties of clusters are known to be size specific[1,14,15] and thus will change upon aggregation. It has generally been found that ozonolysis is superior to thermal treatment for ligand removal, yielding materials with increased resistance to further sintering.[13,16] However, it has been shown that both calcination and ozonolysis treatments result in some degree of cluster aggregation due to the relatively weak gold−oxide interaction.[16]

A number of groups have suggested and explored the use of surface pre-treatments to prevent gold cluster aggregation. Hidalgo et al. have demonstrated that sulfuric acid pre-treatment of TiO_2 leads to the fixation of sulfate groups on the particle surface, resulting in a much stronger support−nanoparticle interaction.[17] Veith et al. have reported that pre-treatment of TiO_2 with both acid and base may help prevent gold nanoparticle aggregation,[18] so the modification of the TiO_2 surface by H^+ in the case of sulfuric acid pre-treatment may also play a role in improving the metal−support interaction. In addition, further studies have shown that hydroxylation of the TiO_2 surface results in a drastic

Received: August 9, 2015
Revised: September 30, 2015
Published: October 1, 2015

DOI: 10.1021/acs.jpcc.5b07732
J. Phys. Chem. C 2015, 119, 24465−24474

improvement in gold cluster catalytic activity while negligibly affecting aggregation.[19] Zhong et al. showed that the addition of Sn^{2+} to the surface of titanium dioxide improved the dispersion of Pd, Pt, Au, and Ag nanoparticles, as well as mixed-metal nanoparticles composed of these elements.[20] Similar systems prepared in the absence of tin experienced aggregation, and it was proposed that strong bonding between tin-hydroxyl chelates and metal clusters was responsible for the high dispersion. Matthey et al. have explored the nucleation of small (<20 atoms) gold clusters on oxidized, reduced, and hydrated TiO_2 surfaces.[21] The authors found that the gold−oxide bond is strongest in the case of an oxidized support, while hydrated TiO_2 surfaces readily allowed aggregation to larger gold particles. This behavior of ultrasmall clusters is in stark contrast to that of larger (∼1.5 nm) gold nanoparticles, which aggregate readily on an oxidized support,[22] especially at higher temperatures.[23]

While the reports mentioned above demonstrate the importance of surface pre-treatment, they are not suited to direct comparison due to the variations in individual approaches toward material fabrication. To our knowledge there has been no comprehensive comparative report on the effect of support pre-treatments on the gold−support interaction. Ideally, one would aim to focus on the effect of support pre-treatment only, but in order to do so it is important to eliminate interference caused by other factors (e.g., type of support, cluster synthesis method) to isolate the effect of pre-treatment methods.

In this report, the effects of a number of pre-treatments on the deposition and activation of atomically precise gold clusters were investigated. We have selected a number of pre-treatment methods (discussed above) that have been proven to affect gold cluster aggregation on metal oxide supports.[17−21] These pre-treatment methods were applied to the commercially available Aeroxide P-25 TiO_2 support (a NIST standard, widely available, and a popular support material in the research community).[24] These pre-treated materials were subsequently used as supports for the $[Au_9(PPh_3)_8](NO_3)_3$ cluster (hereafter referred to as Au_9), and the resultant materials were subjected to two post-deposition treatments: calcination and ozonolysis. Detailed investigation of these materials is carried out using synchrotron X-ray photoelectron spectroscopy (XPS).[6,9] UV−vis diffuse reflectance spectroscopy (UV−vis DRS) was used to give a detailed picture of gold particle aggregation on the support surface via the appearance of the surface plasmon resonance band for particles larger than 2.5 nm.[25,26] Using these techniques in conjunction, we demonstrate the effects of pre-treatment on the behavior of the Au_9 clusters during deposition and activation. By using the exact same support material for each pre-treatment, we eliminate any interference due to variability in nature of the support. The use of P-25 as a support allows the results of this report to be widely applicable, benefiting numerous researchers working in the area by providing a comprehensive reference point.

This report builds on our recent studies on a series of atomically precise clusters deposited and activated on titania, in which we have demonstrated the use of synchrotron XPS for the characterization of cluster-containing materials and also shown a correlation between each clusters' electronic properties and their size.[6,9] Our earlier studies have also highlighted the important role support pre-treatment plays in the aggregation of gold clusters. Here, by using atomically precise Au_9 clusters as a probe sensitive to aggregation, we have been able to focus on exactly how various pre-treatment methods of the same, popular support affect nanoparticle aggregation, both during cluster deposition and upon post-deposition treatments. The fundamental study reported herein is therefore intended to act as a foundation for further studies on the applications of these materials.[25−27] In the proceeding sections we present X-ray photoelectron spectroscopy (XPS) measurements of the gold core, the triphenylphosphine periphery, and the titanium dioxide support, respectively. Following this, we present results of the UV−vis DRS spectroscopy investigations of these (and related) materials, which support the conclusions obtained from XPS data.

EXPERIMENTAL SECTION

Gold clusters were deposited on Aeroxide P-25 (Degussa) titanium dioxide in the following manner (Figure 1):

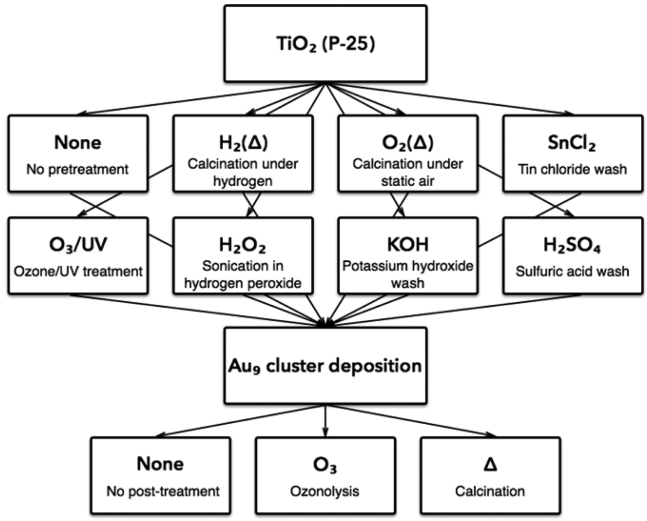

Figure 1. A total of eight predeposition and three post-deposition treatment methods were used, for a total of 24 products. Details of specific treatments are given in the main text.

1. Titanium dioxide was treated using a number of methods, as outlined in the experimental section. Untreated support was also used for comparison. Treatment of the support at this stage will herein be referred to as "pre-treatment".
2. Atomically precise Au_9 clusters were deposited on the titanium dioxide support following a previously reported protocol.[6]
3. Following deposition, Au−TiO_2 systems were treated using either ozonolysis or calcination and were analyzed in comparison to untreated materials. Treatment at this stage will be referred to as "post-treatment".

Materials in this report will be denoted "⟨pre-treatment⟩−TiO_2−⟨post-treatment⟩": e.g. O_3/UV−TiO_2−Δ indicates that the support was ozonolyzed under UV prior to gold cluster deposition and subjected to calcination after the deposition.

Materials. The $AuPPh_3(NO_3)$ gold cluster precursor was synthesized from 99.99% pure gold following a procedure described previously.[6] P25−TiO_2 "Aeroxide" was supplied by Evonik Degussa GmbH. This titania material is a mixture of particles with 80:20 ratio of anatase and rutile phases, with a quoted average particle size of 30 nm and surface area of 50 $m^2 \cdot g^{-1}$. Sodium borohydride (synthetic grade, Merck), potassium

DOI: 10.1021/acs.jpcc.5b07732
J. Phys. Chem. C 2015, 119, 24465−24474

hydroxide (≥85%, Merck), hydrogen peroxide (50% w/w solution, Jasol), sulfuric acid (99%, Orica Chemnet), and tin chloride hydrate (≥98%, Sigma-Aldrich) were used as received.

$[Au_9(PPh_3)_8](NO_3)_3$ Cluster Synthesis. Au_9 clusters were synthesized by a method described by Wen et al.[29] and used extensively by our group.[6,9] Briefly, a solution of $NaBH_4$ (0.072 g, 1.92 mmol) in ethanol (92 mL) was added to a solution of $AuPPh_3NO_3$ (4.000 g, 7.6 mmol) in ethanol (160 mL). After stirring for 2 h, the solution became deep red and was filtered to remove impurities. The filtrate was dried under reduced pressure and the resultant solid dissolved in CH_2Cl_2 (20 mL) and filtered through a sintered glass funnel. Solvent was once again removed under reduced pressure, and the resultant black precipitate was washed with THF (4 × 50 mL) and then hexanes (3 × 50 mL). The precipitate was crystallized from methanol solution by slow diffusion of diethyl ether at 4 °C over approximately 5 days.

Gold clusters were stored at 4 °C in the dark prior to deposition.

Titanium Dioxide Pre-treatment. P-25 titanium dioxide was pre-treated in a number of ways, as described below. Unless otherwise stated, following treatment all samples were washed three times with Milli-Q water and once with ethanol and dried under reduced pressure.

Potassium Hydroxide Wash. KOH aqueous solution (2 M) was added dropwise to a mixture of P-25 (1.000 g) and Milli-Q water (90 mL) until the pH reached 10. The mixture was stirred at 60 °C for 2 h. The product was removed by centrifugation.[17]

Sonication in Hydrogen Peroxide. P-25 (1.000 g) was added to H_2O_2 solution (10 mL, 50% w/w) and sonicated (Elmasonic S30) for 30 min at 30 °C. Sample was recovered by centrifugation and washed with distilled water and ethanol before being dried at room temperature under vacuum.

Calcination under Hydrogen. P-25 (1.000 g) was placed in a quartz boat in a sealed tube furnace (MTI OTF-1200X). The system was purged with argon (MKS 647C multigas controller, Ar flow rate 1.7 $cm^3 \cdot s^{-1}$) and heated to 450 °C. At this point, hydrogen was added to the argon flow (H_2 flow rate 1.7 $cm^3 \cdot s^{-1}$). Gas flow was maintained for 3 h, after which the hydrogen flow was stopped and the sample allowed to cool to room temperature under argon flow. The sample was not washed prior to cluster deposition.

Calcination under Static Air. P-25 (1.000 g) was placed in a quartz boat in a tube furnace, left open to the atmosphere. The sample was heated to 400 °C for 2 h. The sample was not washed prior to cluster deposition.

Ozone/UV Treatment. P-25 (1.000 g) was placed in a quartz tube and stirred under ozone flow (produced using a Yanco Industries OL100DS generator) and UV exposure (provided by a 500 W Ushio UXL-500D-O broad-spectrum Xe lamp) for 2 h. The sample was not washed prior to cluster deposition. The ozone concentration was 129 mg L^{-1} and kept constant for all ozone-treated samples.

Sulfuric Acid Wash. P-25 (1.000 g) was added to sulfuric acid solution (10 mL, 1 M) and stirred for 5 h. Sample was recovered by centrifugation and washed with distilled water followed by methanol before being dried at 100 °C for 16 hours under vacuum.

Tin Chloride Wash. Tin chloride solution ([Sn] = 26.4 mM) was formed by adding $SnCl_2 \cdot 2H_2O$ (1.19 g) to HCl (200 mL, 0.02 M). P-25 (1.000 g) was dispersed in Milli-Q water (200 mL) before being added to the tin chloride solution. The pale yellow suspension was stirred for 10 min, removed from the tin chloride solution by centrifugation, and washed with HCl solution (1 M) five times to remove SnClOH (insoluble at pH 7) formed on its surface.

Gold Cluster Deposition. Gold clusters were deposited on pre-treated P-25 titanium dioxide supports to give a 0.17% metal loading (by mass of Au). In a typical preparation, 1.000 g of titania was dispersed in CH_2Cl_2 (20 mL) with stirring. Au_9 clusters (3.9 mg) were dissolved in CH_2Cl_2 (5 mL) and added to the suspension, and the mixture was stirred for 1 h. Following this, the solvent was removed under reduced pressure. $Au-TiO_2$ products were stored and processed in the absence of light, as exposure to light has previously been shown to encourage cluster aggregation.[18]

Portions of each material were then treated using one of the two different post-deposition treatments (see Figure 1).

Ozonolysis. An amount of 200 mg of sample was stirred under constant ozone flow (Yanco Industries OL100DS) for 90 min, before being washed twice with ethanol and dried under vacuum.

Calcination. An amount of 100 mg of sample was heated in a Schlenk tube to 200 °C under vacuum with stirring for 1 h.

In both cases, care was taken to prevent exposure to light during these post-treatments.

Characterization. X-ray photoelectron spectroscopy (XPS) was performed at the Australian Synchrotron (soft X-ray beamline)[28] using a SPECS Phoibos 150 hemispherical electron analyzer. XPS measurements were performed with an excitation energy of 625 eV and a pass energy of 20 eV. In the XP spectra, all binding energies are referenced to the main carbon peak at 285 eV. The background was fitted using a combination Shirley background/polynomial function. Peaks were fit using pseudo-Voigt peaks fixed at 30% Cauchy (Lorentz) character and 70% Gaussian character. Due to the low gold cluster loading, gold and phosphorus XP spectra were measured ten times and averaged to remove noise and check that no beam-induced aggregation occurred, while other signals of interest were measured twice and averaged. No samples required major correction of the binding energies, indicative of little or no charging of samples.

UV−visible diffuse reflectance spectroscopy (UV−vis DRS) was performed using an Agilent Cary 4000 UV−vis spectrometer with diffuse reflectance sphere. Band gaps were calculated from a modified Kubelka−Munk plot, assuming a direct transition (see Supporting Information, Figure S1 for a typical plot). Background under SPR peaks was approximated using a quadratic function. Peaks were fitted with Gaussian functions and parameters determined by nonlinear least-squares fitting. Peak intensity was measured as the area under the curve. The values of full width at half-maximum (fwhm) for these peaks were systematically approximately 110 nm, with a standard deviation of 17 nm.

RESULTS AND DISCUSSION

We have used electron and optical spectroscopy to analyze the Au_9 clusters deposited on P-25. In the following sections we first briefly review the theory behind XPS binding energy shifts before presenting analysis of Au 4f, P 2p, and Ti 2p XPS data. Following this, we present the analysis of UV−vis DRS data, before finally linking these findings together to form a coherent picture of gold cluster aggregation and ligand removal.

X-ray Photoelectron Spectroscopy. Details of XPS survey scans are available in the Supporting Information.

DOI: 10.1021/acs.jpcc.5b07732
J. Phys. Chem. C 2015, 119, 24465−24474

Unless otherwise noted, peak intensities are reported as a fraction of the titanium 2p total peak intensity. Uncertainty in peak position was qualitatively determined by comparing calculated signals with experimental data. Uncertainy in peak intensity was qualitatively determined from the difference between calculated and experimental data, as a proportion of the total signal.

Effects of Pre- and Post-deposition Treatment on Au XPS. The binding energy of Au cluster 4f electrons observed in the XP spectra is influenced by two effects: the initial state effect and the final state effect. Both effects were described in detail by Borman et al.[29] Briefly, the initial state effect can also be referred to as chemical shift and reflects the oxidation state or the charge state of the atom from which the electron is emitted. The final state effect reflects the de-excitation process of the atom excited by the absorption of the X-ray photon. An atom that exists within a finite structure (such as a metal cluster) cannot relax to the ground state in the same way as an atom that exists within the bulk of the same material. The confined structure also cannot screen the hole created through the emission of the electron as efficiently as the respective bulk material. The relaxation energy is different in both cases. The atom in a finite structure stays longer in the charged state,[29] which shifts observed binding energy of emitted electrons to higher values. The final state effect therefore results in a continuous shift as a function of the cluster size.[6,29] It is important to note that initial and final state effects are difficult to separate because they both result in a shift in binding energy.[30] However, the final state effect also shows a broadening in the fwhm with decreasing size of the cluster,[6] and this phenomenon can potentially be used to identify the nature of the peak shift.

The chemical state of the Au cluster may be affected by the interaction of the Au cluster with the titania substrate. This interaction depends on the nature of the support surface at the site of adsorption (for example, a Au cluster adsorbed onto a defect site will interact differently to one adsorbed onto a defect-free area) and can result in electron transfer to or from the gold particle.[31] The interaction of the Au cluster with the metal oxide substrate could also influence the geometrical structure of the cluster.[30,32]

For Au−TiO_2 materials, gold−titania interactions will lead to an increase in the binding energy of the Au 4f peak as the titania support acts to withdraw electron density from the Au clusters. The final state effect, a result of the cluster size, is generally most prevalent for ultrasmall clusters. This effect can be seen by comparing the Au 4f XPS electron binding energies for Au_8 and Au_9 (~85 eV) with that of Au_{11} (84.6 eV).[6] This effect has also been known to result in a fwhm increase as particle size decreases due to the reduced screening of the hole created through the emission of the electron.[29] For a fuller treatment of initial- and final-state effects on Au cluster XPS binding energies, we direct the reader to the work of Borman et al.[29] and our previous papers.[6,9]

It should be noted that these studies were performed in vacuo, and as such the observations reported may differ somewhat from those for particles studied under atmospheric conditions. Herranz et al. have observed that Au−TiO_2 materials studied by ambient pressure XPS exhibit an upshift in Au 4f peak binding energy of ~0.3−0.4 eV when compared to the same measurements performed in vacuo.[33] This change was attributed to the effect of oxidizing gases; it is anticipated that the imposition of vacuum conditions should not change the structural or electronic properties of gold clusters beyond those overall changes observed by Herranz et al.

Gold clusters were analyzed by XPS, with data normalized and corrected as detailed above. Full gold peak data (intensity and position) are given in Figure 2 (tabulated data are available in the Supporting Information, Table S1; fitting of typical Au XP spectra are available in the Supporting Information, Figures S6−7). The uncertainty in determining peak position is estimated to be approximately 0.1 eV. Some smaller peaks, however, exhibit a larger uncertainty, estimated to be approximately 0.3 eV. This holds for $SnCl_2$−TiO_2−Δ, None−TiO_2−O_3, H_2(Δ)−TiO_2−O_3, and H_2(Δ)−TiO_2−Δ. This larger uncertainty of the peak position does not appreciably affect the interpretation of the following results.

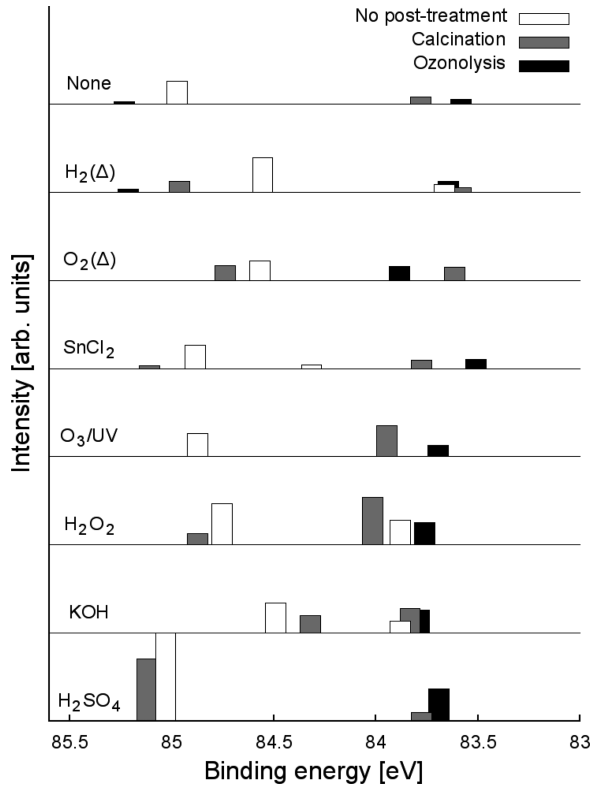

Figure 2. Summary of gold XPS data (binding energy and intensity). Intensity is normalized so that peak heights for different samples are comparable. Post-treatment is indicated by bar shading (see key).

It was observed that Au $4f_{7/2}$ XPS peaks could be broadly divided into two categories: "high binding-energy peaks" (HBP), with a binding energy around 84.5−85.5 eV, and "low binding-energy peaks" (LBP), with a binding energy around 84 eV. Au HBPs are attributed to small discrete gold particles (which may interact with the titania substrate), while Au LBPs are attributed to large (>2 nm) aggregates, whose size results in the emergence of both metallic properties (i.e., a bulk-like Au signal in XPS) and a distinct surface plasmon resonance band.[25,26] Peaks with intermediate binding energies (84−84.5 eV) can be attributed to the small aggregates of clusters. It is also important to note that agglomeration of clusters affects the intensity of the Au signal. Due to the limited electron mean free path, electrons emitted from larger particles will be attenuated more than those emitted from small clusters. The absence of peaks at $E_B \geq 85.5$ eV indicates the absence (within the

DOI: 10.1021/acs.jpcc.5b07732
J. Phys. Chem. C 2015, 119, 24465−24474

detection limit) of surface-bound Au_1 species (e.g., in the form of TiO_2−Au−PPh_3).[34]

Without pre-treatment of support (None−TiO_2), gold clusters aggregate upon either heating or ozonolysis. These results strongly mirror our previous findings.[9] None−TiO_2−Δ shows a very low-intensity HBP around 85.3 eV, approximately 0.5 eV higher than for None−TiO_2−None. The low intensity peak can be attributed to discrete clusters showing interaction with the titania substrate.[6] There is no HBP peak in the case of None−TiO_2−O_3, which indicates complete aggregation of gold clusters for this post-treatment.

Both elevated-temperature pre-treatments (under H_2 and static air) result in a significant decrease in HBP binding energy compared to clusters on untreated TiO_2. Radnik et al. have shown that hydrogen post-treatment of Au−TiO_2 can lower Au 4f electron binding energy.[35] While a similar effect may be postulated for H_2-pre-treated materials, the downward shift observed here may also partly be the result of enhanced cluster-support effects. For both H_2(Δ)−TiO_2 and O_2(Δ)−TiO_2, post-deposition treatments result in the growth of a Au LBP and the shift of the HBP to higher binding energies. This shift in HBP is indicative of considerable cluster deprotection and oxidation (i.e., support interaction). Of note, H_2(Δ)−TiO_2−O_3 is the only ozonolyzed sample to show a Au HBP, suggesting that hydrogen pre-treatment is effective toward immobilization of Au clusters. O_2(Δ)−TiO_2−O_3 appears somewhat resistant toward aggregation as well: the Au LBP has a binding energy approximately 0.4 eV higher than for O_2(Δ)−TiO_2−Δ, indicative of reduced aggregation. It should be noted that the effects observed above are expected to vary based on the particular temperature used in heating the sample: in the results presented here we have specifically avoided exploring the effect of altering the temperature for any given pre-treatment.

Pre-treatment of titania support with tin ($SnCl_2$−TiO_2) appears to have little effect on the nature of deposited Au clusters. $SnCl_2$−TiO_2−None shows a small peak at ∼84.4 eV, which may be due to gold−tin interactions on the support surface. Gold−tin interactions would also explain the relatively high binding energy (∼487 vs 485 eV for metallic tin) of observed Sn 3d XPS peaks (Supporting Information, Figure S2). The Au XPS peak at 84.4 eV disappears upon post-treatments, as does the Sn peak, indicative of the loss of all Sn and all Au-bound Sn. Peak positions and intensities after post-deposition treatment look very similar to those observed for None−TiO_2, suggesting that tin deposition does very little to affect gold cluster aggregation during post-treatments. The one exception is the LBP upon ozonolysis, which is somewhat more intense for $SnCl_2$−TiO_2 than for None−TiO_2.

Support pre-treatment by O_3/UV does not drastically affect gold aggregation in the case of "as-deposited" samples. However, Au XPS peaks for both calcined and ozonolyzed samples appear at higher binding energy and with higher relative intensity than their None−TiO_2 counterparts. This suggests that ozonolysis pre-treatment is effective at limiting the extent of gold cluster aggregation. While hydrogen peroxide pre-treatment results in the appearance of a pronounced Au LBP in the "as-deposited" case (cf. untreated TiO_2), this material retains its HBP after calcination. This suggests H_2O_2 pre-treatment improves gold cluster resistance to aggregation during this post-treatment.

Pre-treatment by KOH washing results in a decrease in the binding energy of the Au HBP for the "as-deposited" sample (cf. None−TiO_2). However, the presence of electron-rich surface TiOH groups is likely to lower the binding energy of deposited Au clusters.[35] A Au LBP is observed for KOH−TiO_2−None, indicating that KOH treatment encourages gold particle aggregation for this particular system, contrary to expectations based on previous reports.[21] Overall, this pre-treatment method does not seem to offer a significant advantage in controlling the aggregation of clusters according to the XPS observations of post-treated samples.

Finally, pre-treatment with H_2SO_4 gives rise to a remarkably intense HBP (the most intense HBP peak observed in this report). The Au XPS peak binding energy is comparable to that of the pure, intact cluster in its solid-state microcrystalline powder form,[6] indicating that the clusters deposited on H_2SO_4−TiO_2 remain intact. Calcination shifts this HBP to a higher binding energy, which is attributed to ligand removal and partial oxidation of the cluster which may be due to a better interaction with the oxide support. A relatively low-intensity LBP is also observed for the calcined sample, indicative of a small population of aggregates. Nonetheless it is noteworthy that the intensity of the HBP of H_2SO_4−TiO_2−Δ is the highest in the series, indicating that support pre-treatment by washing in sulfuric acid is the best approach for preventing aggregation of clusters during calcination. However, ozonolysis post-treatment results in more extensive aggregation, as evidenced by the disappearance of the HBP and the concomitant appearance of an LBP. The high relative intensity of the LBP suggests that these aggregates are still relatively small (albeit already metallic), as a high proportion of Au atoms remains detectable by XPS (compared with other samples in the series).

3.1.2. Effects of Pre- and Post-deposition Treatments on P XPS. The positions of the P 2p XPS are shown in Table 1. The

Table 1. Summary of Phosphorus XPS[a]

pre-treatment	post-treatment	EB [eV] LBP	EB [eV] HBP
None	None	-	134.3
	Heat	-	133.9
	O_3	-	134.1
H_2 (Δ)	None	-	133.4
	Heat	-	134.1
	O_3	-	133.3
O_2 (Δ)	None	-	133.7
	Heat	-	133.7
	O_3	-	134.2
$SnCl_2$	None	-	133.9
	Heat	-	133.7
	O_3	-	133.5
O_3/UV	None	-	134.1
	Heat	-	133.7
	O_3	-	134.3
H_2O_2	None	131.3	133.6
	Heat	-	133.9
	O_3	131.8	134.1
KOH	None	-	133.8
	Heat	-	133.6
	O_3	-	134.3
H_2SO_4	None	131.7	133.3
	Heat	131.6	133.1
	O_3	-	133.7

[a]Peak positions only are shown because the intensity of P was found to depend on the time samples were exposed to vacuum. Binding energies are given to within ±0.2 eV.

DOI: 10.1021/acs.jpcc.5b07732
J. Phys. Chem. C 2015, 119, 24465−24474

intensity of the P peaks are not shown because the intensity depends on the residence time of the samples in vacuum.[10] Triphenylphosphine ligands bound to the Au cluster core display a P 2p XPS peak with binding energy of 131−132 eV.[6] Only four samples—H_2SO_4−TiO_2−None, H_2SO_4−TiO_2−Δ, H_2O_2−TiO_2−None, and H_2O_2−TiO_2−O_3—exhibited this peak (Table 1). The absence of the 131−132 eV P 2p XPS peak shows that the triphenylphosphine ligand periphery was removed even before post-treatment for the majority of pre-treated materials, which correlates with our previous findings.[9] The presence of the P 2p XPS peak with binding energy of 131−132 eV for H_2SO_4 and H_2O_2-pre-treated TiO_2 suggests that these pre-treatment techniques discourage the removal of triphenylphosphine from the cluster core upon deposition. P 2p XPS peaks were observed at 133−134 eV for all samples, which is attributed to oxidized phosphorus most likely bound to the titania surface after detaching from the Au cluster core.[36]

It is believed that the processes of aggregation and ligand removal upon deposition of the cluster onto the substrate are concurrent: this has been observed previously in XPS studies of phosphine-protected gold clusters deposited on titanium dioxide.[6,9] Of particular note, our studies show that gold clusters deposited on untreated commercial P-25 undergo ligand removal and aggregation even without specific post-deposition treatment, confirming reproducibility of our previous findings.[9]

Effects of Pre- and Post-deposition Treatments on Ti-XPS. Relative intensities for all Ti populations are tabulated in the Supporting Information, Table S2, with typical fittings shown in the Supporting Information, Figures S8−9. In all cases, the Ti 2p region displayed two distinct peaks at ∼459.2 and ∼457.6 eV, which correspond to Ti^{4+} and Ti^{3+}, respectively.[37] Ti^{3+} ions in TiO_2 have been known to extend the adsorption of the material into the visible region of the spectrum.[38] Thermal treatment is known to reduce the Ti^{3+} population of TiO_2 materials.[39] The Ti^{3+} population of supports in this study was found to depend on both pre- and post-deposition treatment methods (Figure 3, Supporting Information Table S2). The uncertainty for these values is derived from the difference between calculated and experimental data: variance in the magnitude of this uncertainty is due to either very small Ti^{3+} peaks (e.g., in the case of $SnCl_2$-treated samples) or differences in the amount of signal noise observed for different samples, most probably an artifact of sample preparation.

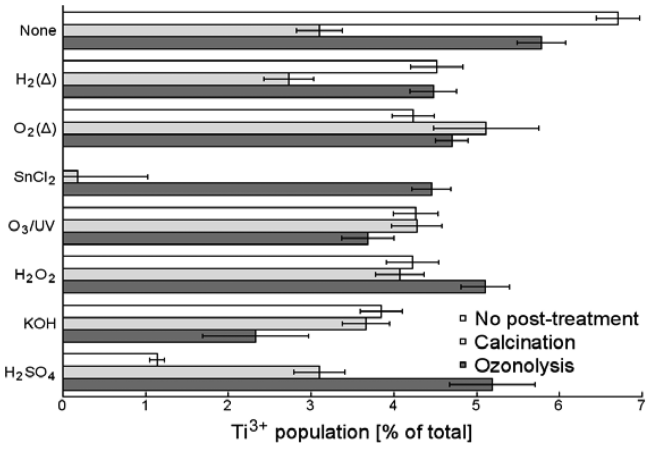

Figure 3. Effect of predeposition and post-deposition treatment method on the percentage of Ti observed in the Ti^{3+} state. $SnCl_2$−TiO_2− None shows no evidence of Ti^{3+}. Error bars indicate 95% C.I.

Untreated P-25 shows the highest recorded Ti^{3+} concentration of all analyzed samples, comparable to previous studies.[40] However, upon calcination the Ti^{3+} population of untreated P-25 support drops drastically (see Figure 3 and Table S2), presumably due to thermally induced reordering of the TiO_2 surface.[39] Ozonolysis, on the other hand, only causes a minor drop in Ti^{3+} population, possibly due to a milder temperature regime during this post-treatment.

Pre-treatment of support at elevated temperature under both hydrogen (reducing) and static air (oxidizing) conditions resulted in reduced Ti^{3+} populations, as has previously been reported[41] (and as was seen for calcination of P-25 under vacuum above). This is likely to be due to thermal reordering and the removal of surface defect sites that could lead to the formation of Ti^{3+} centers.[39] The effect of calcination post-treatment on these samples is varied. The Ti^{3+} population observed for H_2(Δ)−TiO_2−Δ is similar to that of None−TiO_2−Δ, but it appears that static air pre-treatment produces a support with Ti^{3+} population, which is resistant to removal during calcination. Post-treatment by ozonolysis has little to no effect on the Ti^{3+} populations of these samples.

Tin-modified TiO_2 initially displays no peaks due to the Ti^{3+} species (and $SnCl_2$−TiO_2−Δ very little Ti^{3+}), likely due to the electron-withdrawing nature of surface-bound Sn (as detailed above). As tin was removed via post-deposition treatment, the Ti^{3+} population was regenerated. The Sn−TiO_2−O_3, which has the lowest concentration of surface Sn, exhibits a Ti^{3+} population comparable to other samples.

Ozonolysis and hydrogen peroxide pre-treatments were both used in an attempt to form oxide or peroxo species on the surface of the support.[42] Ozonolysis pre-treatment resulted in a decrease in the support Ti^{3+} population which was not regenerated by either calcination or ozonolysis post-deposition treatments. Moreover, ozonolysis post-treatment served only to further decrease the Ti^{3+} population. It is likely that O_3, being a strong oxidizing agent, is able to oxidize a significant proportion of surface Ti^{3+} sites, thus reducing the overall population. Following O_3/UV pre-treatment, calcination has little effect on the Ti^{3+} population of the material. This finding suggests that those Ti^{3+} sites oxidized by predeposition ozonolysis treatment are the same sites that would be removed upon calcination. H_2O_2 pre-treatment resulted in a Ti^{3+} population comparable to O_3/UV−TiO_2, and post-deposition calcination again had little effect on the Ti^{3+} population, suggesting that both H_2O_2 and O_3/UV pre-treatment methods alter the TiO_2 surface in a similar manner. While further ozonolysis on O_3/UV−TiO_2 results in a drop in Ti^{3+} population, H_2O_2−TiO_2−O_3 exhibits an appreciably larger Ti^{3+} population than H_2O_2−TiO_2−None.

Acid and base treatments vary considerably in both the effect on the initial Ti^{3+} populations (in samples which did not undergo post-treatments) and the changes in the Ti^{3+} populations upon post-deposition treatments. H_2SO_4−TiO_2 exhibits a remarkably low Ti^{3+} population, but post-treatment by calcination and ozonolysis both result in considerable recovery. Of note, H_2SO_4−TiO_2−O_3 shows a considerably higher Ti^{3+} population than its nonpost-treated analogue, a trend mirrored by H_2O_2−TiO_2 as discussed above. KOH−TiO_2, however, has a much higher initial Ti^{3+} content which drops significantly upon either post-treatment.

DOI: 10.1021/acs.jpcc.5b07732
J. Phys. Chem. C 2015, 119, 24465−24474

$SnCl_2$-pre-treated materials exhibited a third Ti 2p peak at ~460.1 eV (Supporting Information, Figure S9). Upon ozonolysis, the Sn XPS peak (Supporting Information, Figure S2) greatly decreases in intensity, and the additional Ti peak disappears. This suggests that

1. ozonolysis was effective at removing tin from the surface of the support, and
2. this third Ti peak ($E_B \approx 460$ eV) was caused by interaction with surface-bound tin.

This Ti XPS peak observed at high binding energy is likely due to titanium−oxygen−tin atom interactions on the sample surface, in which tin centers withdraw electron density from titanium.[43]

UV−Vis DRS Analysis. All samples were subject to UV−vis diffuse reflectance spectroscopy (UV−vis DRS) analysis (see Supporting Information, Figure S3 for representative plots). TiO_2 exhibits a strong absorption band for $\lambda < 400$ nm, and the band gap of the material can be approximated from the position and shape of this band using the Kubelka−Munk plot.[44−46] In addition, gold nanoparticles with diameter of 2 nm or greater[26,47] exhibit a broad peak around 400−700 nm due to surface plasmon resonance.[48] The position and intensity of this peak depend on the size and shape of the gold nanoparticles, with larger particles generally giving more intense peaks at higher wavelengths.[48−50] Peak intensity is also a function of gold concentration. Finally, individual Au_9 clusters show a much narrower peak around 480−500 nm due to their electronic structure.[51]

The optical absorption coefficient α of a semiconductor around the band gap can be modeled by the following equation[44−46]

$$\alpha = B\frac{(h\nu - E_g)^{m/2}}{h\nu}$$

where B is a constant; $h\nu$ is the energy of the incident radiation; E_g is the energy of the band gap; and m is a constant set to 1 for direct transitions.[45] By plotting $(\alpha h\nu)^2$ against $h\nu$ is it possible to find the direct band gap, as when $h\nu = E_g$, $\alpha = 0$. Using this method (a typical graph is shown in Figure S1), direct band gap energies were determined for all samples as well as P-25 (Figure 4).

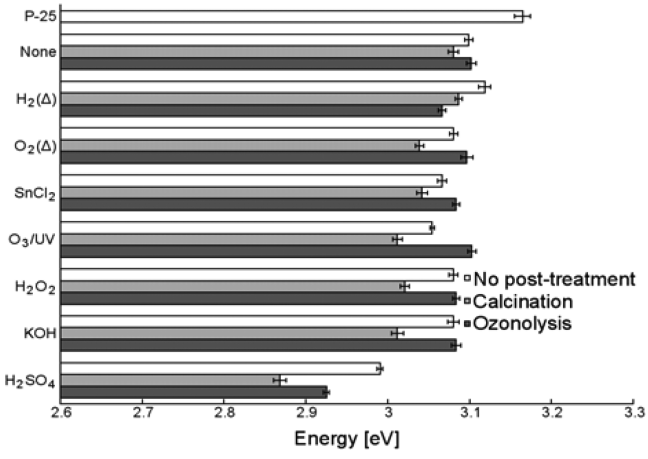

Figure 4. Direct transition band gap energies for Au−TiO_2 materials, with P-25 shown for comparison. Error bars show 95% C.I.

P-25, being ca. 80% anatase, has a band gap of approximately 3.2 eV.[52] Au−TiO_2 samples all show a significantly smaller band gap than pure P-25: this may be due to the influence of Au nanoparticles, but it may also be due to the effect of the treatments.[50] The effect of gold nanoparticle deposition on P-25 can be observed by comparing the band gaps for P-25 and None−TiO_2−None. The band gap diminishes by ca. 0.1 eV upon deposition of the Au clusters. It is observed that while calcination further reduces the band gap of materials ozonolysis either has no effect (H_2O_2−TiO_2, KOH−TiO_2, $O_2(\Delta)$−TiO_2) or widens the band gap ($SnCl_2$−TiO_2, O_3/UV−TiO_2). There are two exceptions to this: $H_2(\Delta)$−TiO_2 and H_2SO_4−TiO_2 both show slight band gap narrowing upon ozonolysis. Observed changes in the bandgap of titania upon pre- and post-treatment may affect the electronic interactions between the Au species and the substrate.[50]

H_2SO_4−TiO_2 materials systematically exhibit the smallest band gaps of the studied materials. This is apparently not due to the lack of Au cluster aggregation, as H_2O_2−TiO_2 (which according to XPS studies above is resistant to aggregation) has a band gap comparable to other samples that exhibited greater aggregation. It may be that the anchoring of sulfate species at the surface enhances visible-light photocatalytic activity, as has been previously reported in the literature.[53,54] Upon calcination, the band gap of H_2SO_4−TiO_2 narrows considerably (from 2.99 to 2.87 eV).

SPR peak positions and intensities are shown in Figure 5. Initial (i.e., before post-treatment) SPR peaks are observed for

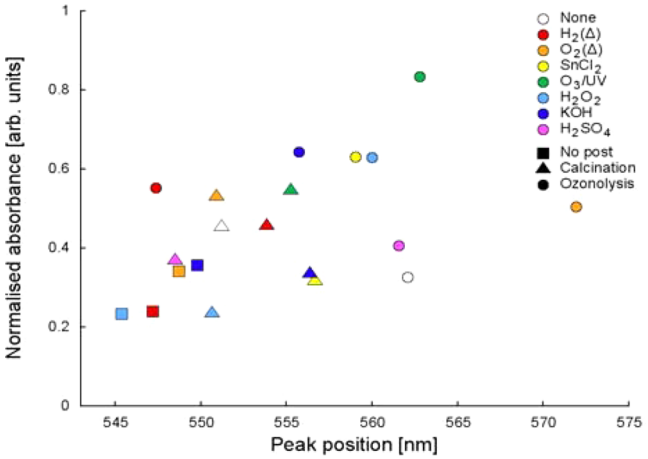

Figure 5. Summary of UV−vis DRS surface plasmon resonance data for Au−TiO_2 samples. Pre-treatments are indicated by the color of the marker, post-treatments by its shape (see key).

H_2O_2−TiO_2, $H_2(\Delta)$−TiO_2, $O_2(\Delta)$−TiO_2, and KOH−TiO_2. This correlates with XPS measurements, which show that these samples exhibit relatively intense Au LBPs (indicative of large gold aggregates) and/or Au HBPs at low binding energies (which suggest that the majority of the gold is present as aggregates). It is interesting that $SnCl_2$−TiO_2−None displays no SPR peak, despite having a small Au LBP at ~84.3 eV. In contrast, $O_2(\Delta)$−TiO_2−None displays an SPR peak despite showing no Au LBP at all. One factor that may influence the presence of SPR peaks is the age of the materials. The materials studied in this report were stored at room temperature in the dark for three months between synthesis/XPS study and UV−vis DRS study, and it may be that even these conditions were enough to result in mild aggregation of clusters on support.[17]

DOI: 10.1021/acs.jpcc.5b07732
J. Phys. Chem. C 2015, 119, 24465−24474

In all cases, the SPR peak becomes more intense and/or shifts to a higher wavelength upon post-deposition treatments, confirming that these treatments result in cluster aggregation. The shift is generally more dramatic upon ozonolysis than calcination, with the exception of $H_2(\Delta)$−TiO_2. This trend agrees with what was observed using Au XPS: thermal pre-treatment of titania under hydrogen enables some of the Au_9 clusters to survive harsh, aggregation-inducing treatment with ozone. The lowest SPR peak position after calcination is observed for H_2SO_4−TiO_2 (∼548 nm), which confirms XPS findings that H_2SO_4−TiO_2 samples were resistant to aggregation during calcination.

Identifying Trends. Au and P XPS and UV−vis DRS data for each sample are summarized in Table 2. In many cases, several observations reinforce one another. For example, samples do not exhibit an SPR peak in the UV−vis DR spectra without an accompanying Au LBP (both indications that a sample contains a sizable population of large, metallic Au particles formed via aggregation of clusters),

Several materials of note will now be highlighted. H_2SO_4−TiO_2−None exhibits the least aggregation of all trialled samples. A high-intensity, high-binding energy Au XPS peak indicates that the clusters have not undergone aggregation, and this is supported by the lack of an SPR peak and the presence of a P XPS peak characteristic of ligands bound to the Au core. All these observations suggest that H_2SO_4-pre-treated TiO_2 prevents ligand removal and aggregation upon deposition, in contrast to untreated TiO_2 (which exhibits no P XPS peak typical of Au-bound ligands and has a less intense, lower-binding energy Au XPS peak). H_2SO_4 pre-treatment also inhibits cluster aggregation upon calcination: this can be seen in the low-wavelength SPR peak (indicative of limited aggregation) and the presence of a high-intensity Au HBP and P XPS ligand peak (indicative of discrete, ligand-protected Au clusters). The majority of phosphorus XPS intensity is observed at the high binding-energy peak (previously ascribed to oxidized phosphorus): this indicates that while protected Au clusters remain on the support surface a significant fraction of those discrete clusters are likely deprotected. Upon ozonolysis the Au HBP disappears, and the SPR peak shifts to higher wavelength. This indicates that ozonolysis of H_2SO_4−TiO_2 results in significant aggregation of gold clusters.

In comparison, $H_2(\Delta)$−TiO_2 exhibits an Au LBP and SPR peak even without post-treatment, suggesting that cluster aggregation occurs even upon deposition. However, the small Au HBP is retained after ozonolysis, and this correlates well with the relatively low wavelength of the $H_2(\Delta)$−TiO_2−O_3 SPR peak. This indicates that the initial aggregation experienced upon gold cluster deposition does not progress markedly upon post-treatment with ozone.

H_2O_2−TiO_2−None shows evidence of retention of discrete clusters as indicated by only a low-wavelength SPR peak, prominent Au HBP, and a small P XPS peak typical for Au-bound ligands. Calcination results in some aggregation (as can be seen by the loss of the P XPS peak due to Au−PPh_3 species and the growth of an Au LBP), but the low-wavelength SPR peak suggests that clusters do not aggregate heavily. Under ozonolysis, even less aggregation occurs, as can be observed by the survival of a small P XPS peak corresponding to Au-bound ligands (although P HBP corresponding to oxidized ligands dominates P XPS) and the presence of a Au HBP. Overall we find a correlation of the shift of the SPR band maxima position and shifts in binding energy of the LBP Au-XPS peaks for all but the $O_2(\Delta)$−TiO_2 sample.

Table 2. Summary of XPS and UV−Vis DRS Data for Au−TiO_2 Materials

pre-treatment	post-treatment: no post-treatment	calcination	ozonolysis
None	DRS: No peak	DRS: SPR peak	DRS: SPR peak
	Au XPS: HBP only	Au XPS: LBP only	Au XPS: Small LBP & HBP
	P XPS: No Au−P peak	P XPS: No Au−P peak	P XPS: No Au−P peak
$H_2(\Delta)$	DRS: SPR peak		
	Au XPS: Small LBP, low-BE HBP	DRS: SPR peak	DRS: Low-λ peak
		Au XPS: Small HBP	Au XPS: HBP still present
	P XPS: No Au−P peak	P XPS: No Au−P peak	P XPS: No Au−P peak
$O_2(\Delta)$	DRS: SPR peak	DRS: Low-λ peak	DRS: High-λ peak
	Au XPS: Small HBP only	Au XPS: Upshifted HBP, LBP	Au XPS: LBP only
	P XPS: No Au−P peak	P XPS: No Au−P peak	P XPS: No Au−P peak
$SnCl_2$	DRS: No peak	DRS: SPR peak	DRS: High-λ peak
	Au XPS: Resembles None−TiO_2	Au XPS: Resembles None−TiO_2	Au XPS: Small HBP/ LBP only
	P XPS: No Au−P peak	P XPS: No Au−P peak	P XPS: No Au−P peak
O_3/UV	DRS: No peak	DRS: SPR peak	DRS: High-λ peak
	Au XPS: Strong HBP only	Au XPS: HBP disappears	Au XPS: LBP only
	P XPS: No Au−P peak	P XPS: No Au−P peak	P XPS: No Au−P peak
H_2O_2	DRS: Low-λ peak	DRS: Low-λ peak	DRS: SPR peak
	Au XPS: HBP and LBP present	Au XPS: Large HBP	Au XPS: High-BE LBP, HBP remains
	P XPS: Small LBP	P XPS: No Au−P peak	P XPS: Small LBP
KOH	DRS: High-λ peak	DRS: High-λ peak	DRS: Low-λ peak
	Au XPS: HBP, LBP present	Au XPS: HBP and LBP downshift	Au XPS: LBP only
	P XPS: No Au−P Peak	P XPS: No Au−P peak	P XPS: No Au−P peak
H_2SO_4	DRS: No peak	DRS: V. low-λ peak	DRS: SPR peak
	Au XPS: V. large HBP only	Au XPS: Large HBP, small LBP	Au XPS: LBP only
	P XPS: Moderate LBP	P XPS: Small LBP	P XPS: No Au−P peak

CONCLUSION

Atomically precise gold clusters were deposited on modified Aeroxide P-25 TiO_2 that had been subjected to a number of popular support pre-treatments. These materials were then treated by either calcination or ozonolysis, mirroring popular ligand removal methods. By using a commercially available support material across these series, we were able to isolate the effects of pre-treatments for the first time, thus providing a widely applicable reference. Synchrotron X-ray photoelectron spectroscopy and UV−vis diffuse reflectance spectroscopy studies provided evidence of both discrete gold clusters and aggregated gold nanoparticles. In the majority of cases, ligand removal takes place upon deposition indicating that post-treatments dedicated to ligand removal are not necessary in such cases.

DOI: 10.1021/acs.jpcc.5b07732
J. Phys. Chem. C 2015, 119, 24465−24474

When compared with pristine TiO_2, it was found that $H_2(\Delta)$, $O_2(\Delta)$, and KOH pre-treatment of the support generally encouraged gold cluster aggregation, while $SnCl_2$, O_3/UV, H_2O_2, and H_2SO_4 support pre-treatments helped to prevent it. Of the pre-treatment methods studied, H_2SO_4 treatment was the most effective at preventing cluster aggregation under calcination, although $H_2(\Delta)$, $O_2(\Delta)$, $SnCl_2$, and O_3/UV pre-treatments also show evidence of retention of the discrete clusters after calcination. $H_2(\Delta)$ pre-treatment was the only method that discouraged cluster aggregation during ozonolysis.

This study clearly demonstrates the importance of support pre-treatment for the control of metal nanoparticle aggregation and provides evidence that pre-treatment with H_2SO_4 and $H_2(\Delta)$ is the most promising means for maintenance of unaggregated clusters under calcination and ozonolysis, respectively.

■ ASSOCIATED CONTENT

Supporting Information

The Supporting Information is available free of charge on the ACS Publications website at DOI: 10.1021/acs.jpcc.5b07732.

Details on X-ray photoelectron spectroscopy and UV−vis diffuse reflectance spectroscopy results, along with typical Kubelka−Munk band gap plots (PDF)

■ AUTHOR INFORMATION

Corresponding Authors

*E-mail: vladimir.golovko@canterbury.ac.nz.
*E-mail: gunther.andersson@flinders.edu.au.
*E-mail: greg.metha@adelaide.edu.au.

Notes

The authors declare no competing financial interest.

■ ACKNOWLEDGMENTS

This research was undertaken on the soft X-ray beamline at the Australian Synchrotron, Victoria, Australia, and supported by funding from NZ Synchrotron Group and Australian Synchrotron (grant AS123/SXR/5335). The authors acknowledge the MacDiarmid Institute, the University of Canterbury, and the New Zealand Ministry of Business, Innovation and Employment (contract number: C05X1207) for funding.

■ REFERENCES

(1) Kartouzian, A.; Thamer, M.; Soini, T.; Peter, J.; Pitschi, P.; Gilb, S.; Heiz, U. Cavity Ring-Down Spectrometer for Measuring the Optical Response of Supported Size-Selected Clusters and Surface Defects in Ultrahigh Vacuum. *J. Appl. Phys.* **2008**, *104*, 124313−8.

(2) Judai, K.; Abbet, S.; Wörz, A. S.; Heiz, U.; Henry, C. R. Low-Temperature Cluster Catalysis. *J. Am. Chem. Soc.* **2004**, *126*, 2732−2737.

(3) Wörz, A. S.; Judai, K.; Abbet, S.; Heiz, U. Cluster Size-Dependent Mechanisms of the Co + No Reaction on Small Pdn (N ≤ 30) Clusters on Oxide Surfaces. *J. Am. Chem. Soc.* **2003**, *125*, 7964−7970.

(4) Valden, M.; Lai, X.; Goodman, D. W. Onset of Catalytic Activity of Gold Clusters on Titania with the Appearance of Nonmetallic Properties. *Science* **1998**, *281*, 1647−1650.

(5) Johnson, G. E.; Wang, C.; Priest, T.; Laskin, J. Monodisperse Au11 Clusters Prepared by Soft Landing of Mass Selected Ions. *Anal. Chem.* **2011**, *83*, 8069−8072.

(6) Anderson, D. P.; Alvino, J. F.; Gentleman, A.; Qahtani, H. A.; Thomsen, L.; Polson, M. I. J.; Metha, G. F.; Golovko, V. B.; Andersson, G. G. Chemically-Synthesised, Atomically-Precise Gold Clusters Deposited and Activated on Titania. *Phys. Chem. Chem. Phys.* **2013**, *15*, 3917−3929.

(7) Chusuei, C. C.; Lai, X.; Davis, K. A.; Bowers, E. K.; Fackler, J. P.; Goodman, D. W. A Nanoscale Model Catalyst Preparation: Solution Deposition of Phosphine-Stabilized Gold Clusters onto a Planar Tio2(110) Support. *Langmuir* **2001**, *17*, 4113−4117.

(8) Bönnemann, H.; Richards; Ryan, M. Nanoscopic Metal Particles − Synthetic Methods and Potential Applications. *Eur. J. Inorg. Chem.* **2001**, *2001*, 2455−2480.

(9) Anderson, D. P.; et al. Chemically Synthesised Atomically Precise Gold Clusters Deposited and Activated on Titania. Part Ii. *Phys. Chem. Chem. Phys.* **2013**, *15*, 14806−14813.

(10) Andersson, G. G.; et al. Phosphine-Stabilised Au9 Clusters Interacting with Titania and Silica Surfaces: The First Evidence for the Density of States Signature of the Support-Immobilised Cluster. *J. Chem. Phys.* **2014**, *141*, 014702.

(11) Lopez-Sanchez, J. A.; et al. Facile Removal of Stabilizer-Ligands from Supported Gold Nanoparticles. *Nat. Chem.* **2011**, *3*, 551−556.

(12) Li, D.; Wang, C.; Tripkovic, D.; Sun, S.; Markovic, N. M.; Stamenkovic, V. R. Surfactant Removal for Colloidal Nanoparticles from Solution Synthesis: The Effect on Catalytic Performance. *ACS Catal.* **2012**, *2*, 1358−1362.

(13) Ho, K. Y.; Yeung, K. L. Effects of Ozone Pretreatment on the Performance of Au/Tio2 Catalyst for Co Oxidation Reaction. *J. Catal.* **2006**, *242*, 131−141.

(14) Kunz, S.; Hartl, K.; Nesselberger, M.; Schweinberger, F. F.; Kwon, G.; Hanzlik, M.; Mayrhofer, K. J. J.; Heiz, U.; Arenz, M. Size-Selected Clusters as Heterogeneous Model Catalysts under Applied Reaction Conditions. *Phys. Chem. Chem. Phys.* **2010**, *12*, 10288−10291.

(15) Heiz, U.; Schneider, W.-D. Size Selected Clusters on Solid Surfaces. *Crit. Rev. Solid State Mater. Sci.* **2001**, *26*, 251−290.

(16) Menard, L. D.; Xu, F.; Nuzzo, R. G.; Yang, J. C. Preparation of Tio2-Supported Au Nanoparticle Catalysts from a Au13 Cluster Precursor: Ligand Removal Using Ozone Exposure Versus a Rapid Thermal Treatment. *J. Catal.* **2006**, *243*, 64−73.

(17) Hidalgo, M. C.; Maicu, M.; Navío, J. A.; Colón, G. Effect of Sulfate Pretreatment on Gold-Modified Tio2 for Photocatalytic Applications. *J. Phys. Chem. C* **2009**, *113*, 12840−12847.

(18) Veith, G. M.; Lupini, A. R.; Dudney, N. J. Role of Ph in the Formation of Structurally Stable and Catalytically Active Tio2-Supported Gold Catalysts. *J. Phys. Chem. C* **2009**, *113*, 269−280.

(19) Veith, G. M.; Lupini, A. R.; Pennycook, S. J.; Dudney, N. J. Influence of Support Hydroxides on the Catalytic Activity of Oxidized Gold Clusters. *ChemCatChem* **2010**, *2*, 281−286.

(20) Zhong, L.-S.; Hu, J.-S.; Cui, Z.-M.; Wan, L.-J.; Song, W.-G. In-Situ Loading of Noble Metal Nanoparticles on Hydroxyl-Group-Rich Titania Precursor and Their Catalytic Applications. *Chem. Mater.* **2007**, *19*, 4557−4562.

(21) Matthey, D.; Wang, J. G.; Wendt, S.; Matthiesen, J.; Schaub, R.; Lægsgaard, E.; Hammer, B.; Besenbacher, F. Enhanced Bonding of Gold Nanoparticles on Oxidized Tio2(110). *Science* **2007**, *315*, 1692−1696.

(22) Chen, M.; Goodman, D. W. Catalytically Active Gold on Ordered Titania Supports. *Chem. Soc. Rev.* **2008**, *37*, 1860−1870.

(23) Biener, J.; Wittstock, A.; Biener, M. M.; Nowitzki, T.; Hamza, A. V.; Baeumer, M. Effect of Surface Chemistry on the Stability of Gold Nanostructures. *Langmuir* **2010**, *26*, 13736−13740.

(24) Thinnes, B. New Nanoscale Reference Material to Be Known as P25. *Hydrocarbon Processing* **2012**.

(25) Ovoshchnikov, D. S.; Donoeva, B. G.; Williamson, B. E.; Golovko, V. B. Tuning the Selectivity of a Supported Gold Catalyst in Solvent- and Radical Initiator-Free Aerobic Oxidation of Cyclohexene. *Catal. Sci. Technol.* **2014**, *4*, 752−757.

(26) Donoeva, B. G.; Ovoshchnikov, D. S.; Golovko, V. B. Establishing a Au Nanoparticle Size Effect in the Oxidation of Cyclohexene Using Gradually Changing Au Catalysts. *ACS Catal.* **2013**, *3*, 2986−2991.

(27) Adnan, R. H.; Andersson, G. G.; Polson, M. I. J.; Metha, G. F.; Golovko, V. B. Factors Influencing the Catalytic Oxidation of Benzyl

DOI: 10.1021/acs.jpcc.5b07732
J. Phys. Chem. C 2015, 119, 24465−24474

Alcohol Using Supported Phosphine-Capped Gold Nanoparticles. *Catal. Sci. Technol.* **2015**, *5*, 1323.
(28) Cowie, B. C. C.; Tadich, A.; Thomsen, L.; et al. The Current Performance of the Wide Range (90–2500 Ev) Soft X-Ray Beamline at the Australian Synchrotron. *AIP Conf. Proc.* **2009**, *1234*, 307−310.
(29) Borman, V.; Pushkin, M.; Tronin, V.; Troyan, V. Evolution of the Electronic Properties of Transition Metal Nanoclusters on Graphite Surface. *J. Exp. Theor. Phys.* **2010**, *110*, 1005−1025.
(30) Roldan Cuenya, B.; Behafarid, F. Nanocatalysis: Size- and Shape-Dependent Chemisorption and Catalytic Reactivity. *Surf. Sci. Rep.* **2015**, *70*, 135−187.
(31) Freund, H.-J.; Pacchioni, G. Oxide Ultra-Thin Films on Metals: New Materials for the Design of Supported Metal Catalysts. *Chem. Soc. Rev.* **2008**, *37*, 2224−2242.
(32) Yoon, B.; Häkkinen, H.; Landman, U.; Wörz, A. S.; Antonietti, J.-M.; Abbet, S.; Judai, K.; Heiz, U. Charging Effects on Bonding and Catalyzed Oxidation of Co on Au8 Clusters on Mgo. *Science* **2005**, *307*, 403−407.
(33) Herranz, T.; Deng, X.; Cabot, A.; Alivisatos, P.; Liu, Z.; Soler-Illia, G.; Salmeron, M. Reactivity of Au Nanoparticles Supported over Sio2 and Tio2 Studied by Ambient Pressure Photoelectron Spectroscopy. *Catal. Today* **2009**, *143*, 158−166.
(34) Yuan, Y.; Asakura, K.; Kozlova, A. P.; Wan, H.; Tsai, K.; Iwasawa, Y. Supported Gold Catalysis Derived from the Interaction of a Au−Phosphine Complex with as-Precipitated Titanium Hydroxide and Titanium Oxide. *Catal. Today* **1998**, *44*, 333−342.
(35) Radnik, J.; Mohr, C.; Claus, P. On the Origin of Binding Energy Shifts of Core Levels of Supported Gold Nanoparticles and Dependence of Pretreatment and Material Synthesis. *Phys. Chem. Chem. Phys.* **2003**, *5*, 172−177.
(36) Moulder, J. F.; Stickle, W. F.; Sobol, P. E.; Bomben, K. D. *Handbook of X-Ray Photoelectron Spectroscopy*; Physical Electronics, Inc.: Eden Prairie, 1995.
(37) Jagadale, T. C.; Takale, S. P.; Sonawane, R. S.; Joshi, H. M.; Patil, S. I.; Kale, B. B.; Ogale, S. B. N-Doped Tio2 Nanoparticle Based Visible Light Photocatalyst by Modified Peroxide Sol−Gel Method. *J. Phys. Chem. C* **2008**, *112*, 14595−14602.
(38) Zuo, F.; Wang, L.; Wu, T.; Zhang, Z.; Borchardt, D.; Feng, P. Self-Doped Ti3+ Enhanced Photocatalyst for Hydrogen Production under Visible Light. *J. Am. Chem. Soc.* **2010**, *132*, 11856−11857.
(39) Amano, F.; Nakata, M.; Asami, K.; Yamakata, A. Photocatalytic Activity of Titania Particles Calcined at High Temperature: Investigating Deactivation. *Chem. Phys. Lett.* **2013**, *579*, 111−113.
(40) Ruzicka, J.-Y.; Bakar, F. A.; Thomsen, L.; Cowie, B. C.; McNicoll, C.; Kemmitt, T.; Brand, H. E. A.; Ingham, B.; Andersson, G. G.; Golovko, V. B. Xps and Nexafs Study of Fluorine Modified Tio2 Nano-Ovoids Reveals Dependence of Ti3+ Surface Population on the Modifying Agent. *RSC Adv.* **2014**, *4*, 20649−20658.
(41) Sanjinés, R.; Tang, H.; Berger, H.; Gozzo, F.; Margaritondo, G.; Lévy, F. Electronic Structure of Anatase Tio2 Oxide. *J. Appl. Phys.* **1994**, *75*, 2945−2951.
(42) Corma, A.; Esteve, P.; Martinez, A.; Valencia, S. Oxidation of Olefins with Hydrogen Peroxide and Tert-Butyl Hydroperoxide on Ti-Beta Catalyst. *J. Catal.* **1995**, *152*, 18−24.
(43) Duan, Y.; Fu, N.; Zhang, Q.; Fang, Y.; Zhou, X.; Lin, Y. Influence of Sn Source on the Performance of Dye-Sensitized Solar Cells Based on Sn-Doped Tio2 Photoanodes: A Strategy for Choosing an Appropriate Doping Source. *Electrochim. Acta* **2013**, *107*, 473−480.
(44) Serpone, N.; Lawless, D.; Khairutdinov, R. Size Effects on the Photophysical Properties of Colloidal Anatase Tio2 Particles: Size Quantization Versus Direct Transitions in This Indirect Semiconductor? *J. Phys. Chem.* **1995**, *99*, 16646−16654.
(45) Sanchez, E.; Lopez, T. Effect of the Preparation Method on the Band Gap of Titania and Platinum-Titania Sol-Gel Materials. *Mater. Lett.* **1995**, *25*, 271−275.
(46) Xu, J.; Liu, Q.; Lin, S.; Cao, W. One-Step Synthesis of Nanocrystalline N-Doped Tio2 Powders and Their Photocatalytic Activity under Visible Light Irradiation. *Res. Chem. Intermed.* **2013**, *39*, 1655−1664.
(47) Esumi, K.; Sarashina, S.; Yoshimura, T. Synthesis of Gold Nanoparticles from an Organometallic Compound in Supercritical Carbon Dioxide. *Langmuir* **2004**, *20*, 5189−5191.
(48) Kowalska, E.; Mahaney, O. O. P.; Abe, R.; Ohtani, B. Visible-Light-Induced Photocatalysis through Surface Plasmon Excitation of Gold on Titania Surfaces. *Phys. Chem. Chem. Phys.* **2010**, *12*, 2344−2355.
(49) Sonawane, R. S.; Dongare, M. K. Sol−Gel Synthesis of Au/Tio2 Thin Films for Photocatalytic Degradation of Phenol in Sunlight. *J. Mol. Catal. A: Chem.* **2006**, *243*, 68−76.
(50) Tian, B.; Zhang, J.; Tong, T.; Chen, F. Preparation of Au/Tio2 Catalysts from Au(I)−Thiosulfate Complex and Study of Their Photocatalytic Activity for the Degradation of Methyl Orange. *Appl. Catal., B* **2008**, *79*, 394−401.
(51) Wen, F.; Englert, U.; Gutrath, B.; Simon, U. Crystal Structure, Electrochemical and Optical Properties of [Au9(Pph3)8](No3)3. *Eur. J. Inorg. Chem.* **2008**, *2008*, 106−111.
(52) Diebold, U. The Surface Science of Titanium Dioxide. *Surf. Sci. Rep.* **2003**, *48*, 53−229.
(53) Colón, G.; Hidalgo, M. C.; Munuera, G.; Ferino, I.; Cutrufello, M. G.; Navío, J. A. Structural and Surface Approach to the Enhanced Photocatalytic Activity of Sulfated Tio2 Photocatalyst. *Appl. Catal., B* **2006**, *63*, 45−59.
(54) Yang, Q.; Xie, C.; Xu, Z.; Gao, Z.; Du, Y. Synthesis of Highly Active Sulfate-Promoted Rutile Titania Nanoparticles with a Response to Visible Light. *J. Phys. Chem. B* **2005**, *109*, 5554−5560.

DOI: 10.1021/acs.jpcc.5b07732
J. Phys. Chem. C 2015, 119, 24465−24474